The International Journal of Advanced Manufacturing Technology (2019) 102:1215–1225
https://doi.org/10.1007/s00170-018-2949-y

ORIGINAL ARTICLE

Stability of turning process with a distributed cutting force model

Yonglin Wu[1] · Qinghua Song[1,2] · Zhanqiang Liu[1,2] · Bing Wang[1]

Received: 11 June 2018 / Accepted: 29 October 2018 / Published online: 5 November 2018

Abstract
Chatter is investigated for a single degree of freedom model of turning process, where the tool is simplified into a cantilever beam, and the modal parameters of the tool can be obtained from the theory of continuous beam. The cutting force is modeled as a force system distributed along the rake face of the tool. And the distributed cutting force combines the Taylor approximation of the cutting force with an exponential shape function. The distributed cutting force model results in a discrete time delay and a continuous time delay in the governing equation of the system, while the conventional cutting force model only involves a discrete time delay. It is shown that the delay terms significantly influence the stability of machining operations, especially at low spindle speeds. The effect of the continuous time delay is further studied in this paper by ignoring the discrete time delay in the governing equations of the system. The semi-discretization technique is used to compute the stability lobe diagrams of turning operations. The sensitivity of stability charts to the shape of force distribution and the ratio of the discrete time delay and the continuous time delay q is analyzed. Turning stability tests are also conducted to verify the accuracy of the distributed cutting force model.

Keywords Stability · Distributed cutting force · Turning · Discrete time delay · Continuous time delay

1 Introduction

Turning is the most widely used machining process and mainly produces different products by cutting metal. In the process of cutting metal, there is an unstable relative vibration between cutting tools and workpieces, which is chatter. The occurrence of chatter during metal cutting processes is an important problem in manufacturing technology. Chatter has a lot of unfavorable effects: it reduces the productivity and the surface quality, causes noise, reduces the life of machine tool and cutting tool, and even leads to tool damage in some cases. Therefore, it is highly necessary to avoid chatter for the machine tool industry.

In the past half century, considerable researches have been conducted to study the governing physical phenomena behind chatter in order to understand its nature and describe methods to avoid it. One of the most widely accepted explanations of machine tool chatter is the theory of surface regeneration [1, 2]: the machined surface becomes wavy due to the relative vibrations between the tool and the workpiece. Therefore, delay effects appear in the models of metal cutting operations since the cutting force is determined by the chip thickness, which depends both on the actual tool position and the delayed position at the previous cut. Hence, the delay-differential equations are used to describe machine tool vibrations, and the regenerative machine tool chatter can be considered as the manifestation of self-excited oscillations in a time-delay system. After the theory of surface regeneration, process damping was studied in stability determination in the processes of turning, which is an energy dissipation mechanism at low speeds [3, 4]. An alternative physical explanation for process damping is the distributed cutting force model, which distributed over the tool–chip interface. A distributed force and continuous delay model was improved for stability analysis of low-speed turning, in contrast to the conventional approach, which uses a point force acting at the

✉ Qinghua Song
ssinghua@sdu.edu.cn

Yonglin Wu
wuynlin@163.com

Zhanqiang Liu
melius@sdu.edu.cn

Bing Wang
sduwangbing@sdu.edu.cn

[1] Key Laboratory of High Efficiency and Clean Mechanical Manufacture, Ministry of Education, School of Mechanical Engineering, Shandong University, Jinan, People's Republic of China

[2] National Demonstration Center for Experimental Mechanical Engineering Education, Shandong University, Jinan, People's Republic of China

tool tip [5]. A continuous delay model was given to analyze stability of turning process at low cutting speeds by assuming an alternative physical explanation for process damping where a distributed cutting force model, along with a function distribution over the tool–chip interface [6]. The abovementioned researches have laid foundations for the analysis of chatter in machining processes.

In recent years, the issue of turning stability has become the focus of many scholars, and a large number of researches have been carried out. Molnar et al. [7] proposed the bistable zone for machining operations, which is estimated for the case of a distributed cutting force model. Huang et al. [8] presented a method for investigating the probabilistic analysis of the regenerative chatter stability in turning by using the Monte Carlo simulation method and advanced first-order second-moment method. Insperger et al. [9] proposed a model of turning operations with state-dependent distributed time delay by applying the theory of regenerative machine tool chatter and describing the dynamics of the tool–workpiece system during cutting by delay differential equations. Ozturk et al. [10] formulated stability of parallel turning processes in frequency and time domain for two different parallel turning cases to determine chatter-free cutting process parameters. Gyebrószki et al. [11] proposed a combined model of the surface regeneration effect and chip formation to predict the stability of turning processes. Comak et al. [12] proposed a general mathematical model to predict the chip thickness, cutting force, and chatter stability of turn milling operations. However, most of these studies either ignore the effect of distributed cutting forces on turning stability or only use the distributed cutting force and the point cutting force to compare the difference in stability analysis of turning, they do not illustrate exactly what the impact of distributed cutting force is in the stability analysis of turning.

The cutting force models began to appear in literature about half a century ago [13, 14, 15]. Many models have been proposed to characterize the cutting forces as a function of the cutting parameters, such as the instantaneous chip thickness and the depth of cut whose product forms the instantaneous chip area. These models treated cutting forces as a point force, which acts at the tool tip. This conventional approximation of the cutting forces has been verified experimentally in the middle range of cutting speeds. However, actual observations of the cutting process at low speeds show improved stability when compared with those obtained from theoretical predictions. The concentrated force model cannot reflect the realistic representation of the physical cutting forces at low cutting speeds. Due to many machining operations that can be carried out only at low speeds [16], it is necessary to put forward a new cutting force model to solve the problem. Thus, many scholars have proposed a distributed cutting force model for the analysis of turning stability based on the actual contact between tool and workpiece. The distributed cutting force model has a great impact on low-speed cutting stability, which reflects a more realistic representation of the physical cutting forces. The distributed cutting force model results in a discrete time delay and a continuous time delay in the governing equation of the system, while the conventional cutting force model only involves a discrete time delay.

According to the references [17, 18], there are two main analytic methods to solve the natural frequencies of cantilever beams. One of the analytic methods is the lumped-parameter system, the other is the continuous system. A lumped-parameter system can be considered to be a system consisting of point masses separated by springs and dampers. The parameters of the system are discrete sets of finite numbers. On the other hand, in a continuous system, the mass, elasticity (or flexibility), and damping are distributed throughout the system. During vibration, each of the infinite number of point masses moves relative to each other's point mass in a continuous fashion. The choice of modeling a given system as discrete or continuous depends on the purpose of the analysis and the expected accuracy of the results. For a continuous system, the governing equation of motion is in the form of a partial differential equation. Since the solution of a set of ordinary differential equations is simple, it is relatively easy to find the response of a discrete system that is experiencing a specified excitation. On the other hand, solution of a partial differential equation is more involved, and closed-form solutions are available for only a few continuous systems that have a simple geometry and simple boundary conditions and excitations.

In this paper, the so-called surface regeneration effect [19] is followed to have the further results on the more accurate modeling of machine tool chatter. Firstly, the tool is simplified to a continuous cantilever beam to analyze the modal parameters. Secondly, the stability analysis of turning processes is investigated by taking the distributed cutting force model into account. In the process of stability analysis, the distributed cutting force model includes both a discrete time delay and a continuous time delay, which has a great impact on low-speed cutting stability. Here, the distributed cutting force model is extended to turning processes and perform the stability analysis, where the discrete time delay is negligible to illustrate exactly the impact of the distributed cutting force. The semi-discretization technique [20, 21] is used to chart the stability boundaries for turning operation. Lastly, external turning operations are performed to verify the accuracy of the proposed model.

2 Mechanical model

In the section, a single degree of freedom model of turning process is investigated (as shown in Fig. 1). The governing equation of motion for a rigid workpiece and a tool compliant in one direction, $x(t)$, is:

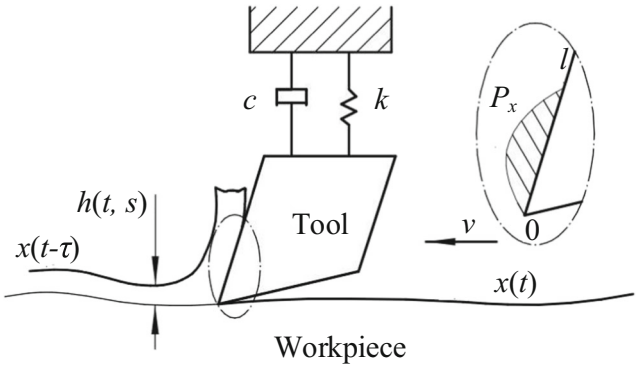

Fig. 1 Schematic diagram of turning process with a distributed force model

$$m\ddot{x}(t) + c\dot{x}(t) + kx(t) = F_x(t) \tag{1}$$

Where m, c, and k are the modal mass, damping, and stiffness parameters, respectively, and $F_x(t)$ is the x-directional cutting force component acting on the tool.

2.1 Calculation of tool modal parameters

In order to solve the governing equation of motion, it is necessary to calculate the tool modal parameters. In the process of turning large diameter solid workpieces, cutting chatter mainly occurs on cutting tools, because the stiffness of workpiece is larger than that of the tool. The tool can be simplified to a cantilever beam with one end fixed and one end free during the modeling process. The cantilever beam has a simple geometry and simple boundary conditions. Moreover, the accuracy of the natural frequencies can be improved by using the continuous system. Therefore, the cantilever beam is assumed as a continuous system with infinite degrees of freedom. In other words, there are infinite natural frequencies and natural modes.

In the process of turning, the bending of the tool is mainly caused by bending moment. Thus, for the sake of convenience, the Euler-Bernoulli beam theory [22] is used to calculate the first three order modal parameters of the tool, which ignores the shear deformation. Assuming that the tool is a uniform beam, the differential equation of motion of tool is:

$$EI\frac{\partial^4 w(x,t)}{\partial x^4} + \rho A\frac{\partial^2 w(x,t)}{\partial t^2} = 0 \tag{2}$$

If the tool is fixed at $x = 0$ and free at $x = e$ (e is the overhang length of tool), the transverse deflection and its slope must be 0 at $x = 0$, and the bending moment and shear force must be 0 at $x = e$. Thus, the boundary conditions are:

$$w(0) = 0, \frac{dw}{dx}(0) = 0, \frac{d^2w}{dx^2}(e) = 0, \frac{d^3w}{dx^3}(e) = 0 \tag{3}$$

So, the natural frequency of the vibration system:

$$w_n = (\beta_n e)^2\left(\frac{EI}{\rho V e^4}\right)^{1/2}, n = 1, 2, 3\ldots \tag{4}$$

Where, β_n is the calculation coefficient of the natural frequency; E is the modulus of elasticity of the tool; I is the moment of inertia of the tool; ρ is the density of the tool; V is the sectional area of the tool $V = r \times j$; r is the width of the cutter; and j is the height of the cutter. And, hence the nth mode shape can be expressed as:

$$W_n(x) = C_{1n}\left[(\cos\beta_n x - \cosh\beta_n x) - \frac{\cos\beta_n e + \cosh\beta_n e}{\sin\beta_n e + \sinh\beta_n e}(\sin\beta_n x - \sinh\beta_n x)\right] \tag{5}$$

The size and material properties of the tool are shown in Table 1.

By submitting the parameters of Table 1 into Eq. (4), the three first-order natural frequencies of the cutting tool can be obtained: $\omega_1 = 1704.1$ Hz; $\omega_2 = 10{,}680.0$ Hz; $\omega_3 = 29{,}907.1$ Hz.

In order to verify the correctness of the natural frequencies obtained by the Euler-Bernoulli beam theory, a hammer mode experiment is conducted to obtain the natural frequency of the tool, which is a necessary element to draw the stability lobe diagram. In the hammer mode experiment, a hammer is used to hit the tool that is clamped on a CNC lathe, and an accelerometer with a sensitivity of 98.45 mv/g is used to collect signals. Due to the limitation of the modal parameter extraction method, the hammer and accelerometer must be in the form of "point-to-point" percussion. The hammer mode experiment setup is shown in Fig. 2. The rest of the equipment includes a B&K data acquisition box and a matching computer.

Through the hammer mode experiment, the first-order natural frequency ω_1 is 1574.2 Hz, which is very close to the first-order natural frequency (1704.1 Hz) obtained by the Euler-Bernoulli beam theory.

2.2 Distributed cutting force model

In the process of turning, the tool and the workpiece are in contact with each other on the front, edge, and back of the tool; so, it is impossible that the practical cutting force is a concentrated point force. Compared with the conventional point cutting force, the distributed force model reflects a more realistic representation of the physical cutting forces in turning. Besides, the distributed force model also provides an

Table 1 Size and material properties of the tool

r (m)	j (m)	e (m)	E (GPa)	ρ (kg/m^3)
0.025	0.025	0.11	206	7900

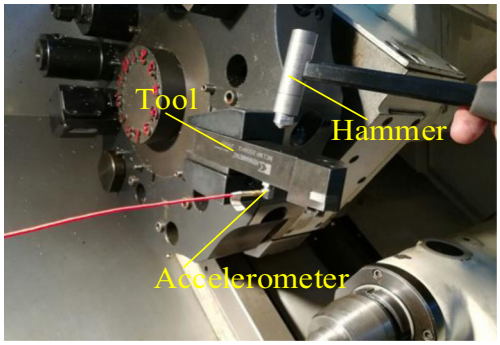

Fig. 2 The hammer mode experiment setup

alternative explanation for the improved stability at low speeds. Therefore, the construction of distributed cutting force model is of great significance to the study of the stability of turning process. Instead of cutting forces concentrating on a single point on the tool tip, these forces are assumed to have a distribution per unit length p with varying magnitudes along the tool–chip interface, as shown in Fig. 1. The cutting force $F_x(A)$ can be modeled as the resultant of a distributed force system $P_x(A,s)$ on the contact area l between the rake face and chip [23, 24].

$$F_X(A) = \int_0^l P_x(A,s)ds \tag{6}$$

Where s is the distributed delay, which expresses the chip contacting with the rake face of the tool. The local coordinate l whose origin is fixed on the tip of the tool is used to describe the contact distance between the sliding chip and the active face of the tool. The value of l ranges from 0 to the length that represents the position where the chip leaves from the tool. $P_x(A,s)$ is composed of a time-dependent magnitude $F^T{}_x(A)$ and a time-independent shape function $W_x(s)$ [25]:

$$P_x(A,s) = F_x^T(A)W_x(s), s\in[0,l] \tag{7}$$

With the constraint:

$$\int_0^l W_x(s)ds = 1 \tag{8}$$

It is necessary to choose a proper function $F^T{}_x(A)$, which characterizes the magnitude of the cutting force distribution. In the past half century, a lot of cutting experiments and cutting simulations have been carried out to determine the force magnitude $F^T{}_x(A)$. For the cutting force distribution magnitude $F^T{}_x(A)$, there are two kinds of expressions that are more widely applied, one is Taylor force [26], the other is Tobias force [27]. But other kinds of force expressions also exist (see Refs. [28, 29]). In this paper, Taylor's formula is used:

$$F_X^T(A) = \phi(u)KA \tag{9}$$

Where, $\varphi(u)$ is a value 1 when the tool is cutting the workpiece and 0 when the tool leaves the workpiece. K is the cutting coefficient and is usually determined by experiment. A is the instantaneous chip area.

Now, focus on the choice of the weight function $W_x(s)$, which characterizes the shape of cutting force distribution along the rake face of the tool. There are five kinds of widely accepted shapes for the distributions of the normal and the shear stress, which are sine weight function, cosine weight function, constant weight function, exponential weight function, and compound trigonometric weight function (as shown in Fig. 3) [30, 31, 32]. The formulae of these three weight functions are as follows:

1. Sine weight function

$$W_x(s) = \frac{\pi}{2l}\sin\left(\frac{\pi}{l}s\right), s\in[0,l] \tag{10}$$

2. Cosine weight function

$$W_x(s) = \frac{1}{l}\left[1+\cos\left(\frac{\pi}{l}s\right)\right], s\in[0,l] \tag{11}$$

3. Exponential weight function

$$W_x(s) = \frac{1}{l}\exp\left(-\frac{s}{l}\right), s\in[0,\infty] \tag{12}$$

4. Constant weight function

$$W_x(s) = \frac{1}{l}, s\in[0,l] \tag{13}$$

5. Compound trigonometric weight function

$$W_x(s) = \frac{\pi}{2l}\sin\left(\frac{\pi}{l}s+\phi\right), s\in[0,l] \tag{14}$$

It is important to choose a suitable shape function $W_x(s)$, because the more appropriate $W_x(s)$ is selected, the more

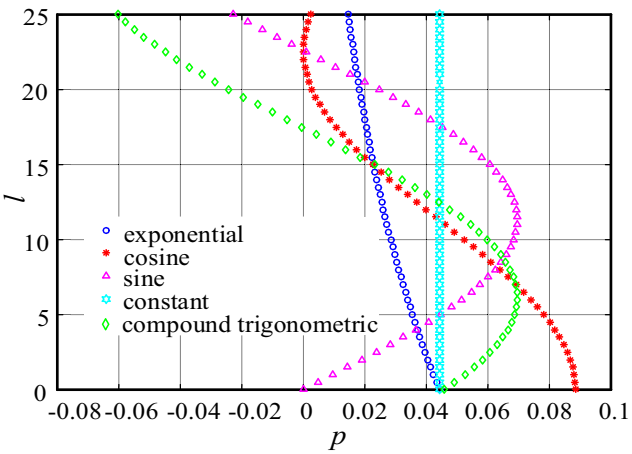

Fig. 3 The weight functions of distributed cutting force

accurate results can be obtained. According to many studies, which showed that the forces over the rake face vary exponentially, thus, in this paper, the shape function $W_x(s)$ is approximated by the exponential function.

Therefore, when the tool is cutting the workpiece, submitting above results, Eqs. (9) and (12) into Eq. (6), yields:

$$F_X(A) = \int_0^l P_x(A,s)ds = \int_0^l F_x^T(A)W_x(s)ds = \int_0^l \phi(u)KA\frac{1}{l}\exp\left(-\frac{s}{l}\right)ds \quad (15)$$

2.3 The equation of motion

Equation (1) can be divided by m and written as:

$$\ddot{x}(t) + 2\xi\omega_n\dot{x}(t) + {\omega_n}^2x(t) = \frac{1}{m}F_x(t) \quad (16)$$

Where $\omega_n = \sqrt{k/m}$ is the natural angular frequency of undamped system and $\xi = c/\sqrt{km}$ is the damping ratio.

Substituting Eq. (15) into Eq. (16) yields:

$$\ddot{x}(t) + 2\xi\omega_n\dot{x}(t) + {\omega_n}^2x(t) = \frac{1}{m}\int_0^l \phi(u)KA\frac{1}{l}\exp\left(-\frac{s}{l}\right)ds \quad (17)$$

When the tool is cutting the workpiece, the cutting force is proportional to the chip area, and the chip area is the product of cutting width and cutting thickness. Hence, the chip area A is:

$$A = b(h(t,s) - h_0) \quad (18)$$

Where b is the chip width, h_0 is the mean chip thickness, and $h(t,s)$ is the instantaneous chip thickness.

According to the theory of regenerative machine tool vibrations, the instantaneous chip thickness $h(t,s)$ can be written as a function of the tool position at the actual and the prior cut:

$$h(t,s) = h_0 + x(t-\tau-s) - x(t-s), s\in[0,l] \quad (19)$$

Where τ is the discrete time delay, which is associated with the tool passage period: $\tau = 2\pi/\Omega$.

Submitting Eqs. (18) and (19) into Eq. (17) yields:

$$\ddot{x}(t) + 2\xi\omega_n\dot{x}(t) + {\omega_n}^2x(t) = \frac{\phi(u)Kb}{m}\int_0^l \frac{1}{l}\exp\left(-\frac{s}{l}\right)[x(t-s) - x(t-\tau-s)]ds \quad (20)$$

By substituting $u = vt$ into Eq. (20), then the equation can be transformed into the following form:

$$\frac{d^2x(u)}{du^2} + \frac{2\xi\omega_n}{v}\frac{dx(u)}{du} + \left(\frac{\omega_n}{v}\right)^2x(u) - \frac{\phi(u)Kb}{mv^2}\int_0^l \frac{1}{l}\exp\left(-\frac{s}{l}\right)[x(u-s) - x(u-\tau-s)]ds = 0 \quad (21)$$

The integrodifferential form of Eq. (21) with distributed cutting force model includes the discrete time delay due to the tool passage period, as well as the continuous time delay due to the chip sliding over the tool–chip interface, which makes the stability of the system more complex. For the choice of the shape functions, the more realistic exponential weight function is selected after comparing sine weight function, cosine weight function, exponential weight function, constant weight function, and compound trigonometric weight function. In the same way, Taylor's formula is selected as the suitable force magnitude ${F^T}_x(A)$.

3 Stability analysis

In this section, Eq. (21) is transformed into the state-space equation, which can be used to study the stability analysis of the system by using the semi-discretization method. The analysis is shown for the distributed force model, which includes the short time delay and the long time delay, and a similar analysis can be used for the distributed force model, which only includes the short time delay. As a result, stability boundaries are plotted for continuous steady turning process.

By introducing dimensionless parameter:

$$\tilde{u} = \frac{u}{d\pi} \quad (22)$$

And the angular velocity:

$$n = \frac{2\pi}{v} \quad (23)$$

Eq. (21) can be written as:

$$x^{(2)}\left(\tilde{u}\right) + 2\xi\omega_n\frac{2\pi}{n}x^{(1)}\left(\tilde{u}\right) + \left(\frac{2\pi\omega_n}{n}\right)^2x\left(\tilde{u}\right) - \frac{\phi\left(\tilde{u}\right)kb}{m}\int_0^{1/q}\frac{1}{l}\exp\left(-\frac{\tilde{s}}{l}\right)\left(x\left(\tilde{u}-\tilde{s}\right) - x\left(\tilde{u}-1-\tilde{s}\right)\right)d\tilde{s} = 0 \quad (24)$$

Where the new parameter is described as:

$$q = \frac{d\pi}{l} \quad (25)$$

Transform variable s to the new variable θ:

$$W_x\left(\tilde{s}\right) = \frac{1}{l_0}\exp\left(-\frac{\tilde{s}}{l_0}\right) \Rightarrow W_x(-\theta) = q_0\exp(-q_0\theta), \theta\in[-\infty, 0] \quad (26)$$

Where l_0 can be thought of as the measure of the short time delay; q_0 is defined as $d\pi/l_0$, which is the ratio of the long time delay and the short time delay in the system.

Submitting Eq. (26) into Eq. (24) yields:

$$x^{(3)}\left(\tilde{u}\right) + \left(q_0 + 2\xi\omega_n\frac{2\pi}{n}\right)x^{(2)}\left(\tilde{u}\right) + \left(2\xi\omega_n q_0\frac{2\pi}{n} + \left(\frac{2\pi\omega_n}{n}\right)^2\right)x^{(1)}\left(\tilde{u}\right) + \left({\omega_n}^2 + \frac{\phi\left(\tilde{u}\right)kb}{m}\right)\left(\frac{2\pi}{n}\right)^2 q_0 x\left(\tilde{u}\right) - \frac{\phi\left(\tilde{u}\right)}{m}\left(\frac{2\pi}{n}\right)^2 q_0 x\left(\tilde{u}-1\right) = 0 \quad (27)$$

Which can be written in state-space form as:

$$\begin{bmatrix}\dot{x}_1\left(\tilde{u}\right)\\ \dot{x}_2\left(\tilde{u}\right)\\ \dot{x}_3\left(\tilde{u}\right)\end{bmatrix} = \begin{bmatrix}0 & 1 & 0\\ 0 & 0 & 1\\ -\left({\omega_n}^2 + \frac{\phi\left(\tilde{u}\right)kb}{m}\right)\left(\frac{2\pi}{n}\right)^2 q_0 & -\left(2\xi\omega_n q_0\frac{2\pi}{n} + \left(\frac{2\pi\omega_n}{n}\right)^2\right) & \left(q_0 + 2\xi\omega_n\frac{2\pi}{n}\right)\end{bmatrix}\times \begin{bmatrix}x_1\left(\tilde{u}\right)\\ x_2\left(\tilde{u}\right)\\ x_3\left(\tilde{u}\right)\end{bmatrix} + \begin{bmatrix}0 & 0 & 0\\ 0 & 0 & 0\\ \frac{\phi\left(\tilde{u}\right)}{m}\left(\frac{2\pi}{n}\right)^2 q_0 & 0 & 0\end{bmatrix}\begin{bmatrix}x_1\left(\tilde{u}-1\right)\\ x_2\left(\tilde{u}-1\right)\\ x_3\left(\tilde{u}-1\right)\end{bmatrix} \quad (28)$$

The state-space Eq. (28) could be written in an equivalent form as:

$$\dot{X}\left(\tilde{u}\right) = B\left(\tilde{u}\right)X\left(\tilde{u}\right) + C\left(\tilde{u}\right)X\left(\tilde{u}-1\right) \quad (29)$$

This model involves the distributed cutting force model, which contains the short time delay and the long time delay. The parameter q has an important role in the stability investigation. It can be expressed by means of distances: it is the ratio of the circumference $d\pi$ of cylindrical workpiece and the length l of the contact line of chip and the active face of the tool [33, 34]. When the long time delay effect is negligible, i.e., $q = 0$, the ordinary differential equation of a simple damped oscillator can be transformed into the following form:

$$x^{(3)}\left(\tilde{u}\right) + 2\xi\omega_n\frac{2\pi}{n}x^{(2)}\left(\tilde{u}\right) + \left(\frac{2\pi\omega_n}{n}\right)^2 x^{(1)}\left(\tilde{u}\right) = 0 \quad (30)$$

Which can be written in state-space form as:

$$\begin{bmatrix}\dot{x}_1\left(\tilde{u}\right)\\ \dot{x}_2\left(\tilde{u}\right)\\ \dot{x}_3\left(\tilde{u}\right)\end{bmatrix} = \begin{bmatrix}0 & 1 & 0\\ 0 & 0 & 1\\ 0 & -(2\pi\omega_n/n)^2 & 2\xi\omega_n(2\pi/n)\end{bmatrix}\begin{bmatrix}x_1\left(\tilde{u}\right)\\ x_2\left(\tilde{u}\right)\\ x_3\left(\tilde{u}\right)\end{bmatrix} \text{ or } \dot{X}\left(\tilde{u}\right) = D\left(\tilde{u}\right)X\left(\tilde{u}\right) \quad (31)$$

The stability analysis of the resulting state-space equations is then performed using the numerical analysis method. In this method, the main point of the semi-discretization technique is to approximate the solution operator of the infinite-dimensional delayed system by a large but finite dimensional matrix. The delayed terms are discretized, while the current terms are unchanged and the time-periodic coefficients are approximated by piecewise constant functions [35].

4 Results and discussion

4.1 Experimental verification

According to first-order natural frequency and mode shape of the cutting tool, the modal mass, damping, and stiffness parameters can be obtained. The ratio q_0 can be obtained by the measurement of the diameter of the workpiece and the length l, which is the contact length of chip and the rake face of tool. The length l can be acquired by the following equation:

$$l = \eta z \quad (32)$$

Where η is the ratio of wearing length and contact length, z is the wearing length of the tool's front face. $\eta = 1.67$–3.33 in this paper [36, 37].

As a result, the stability chart for the distributed force model including the short time delay and the long time delay in continuous turning process by using the calculating parameters of Table 2 is shown in Fig. 4.

As shown in Fig. 4, the stability chart tends to shift upward at low cutting speeds, which is attributed to the interference of

Table 2 The calculating parameters

m (kg)	ω_n (Hz)	ζ	q_0
40	1704.1	0.05	22.6

the tool flank with the wavy surface of the workpiece. The energy dissipation through this interference mechanism is called process damping: the increased stability is due to an additional damping force inversely proportional to the spindle speed. An alternative physical explanation for process damping is the distributed cutting force model, which is modeled as the resultant of a force system distributed along the rake face of the tool. Since the chip needs a finite time to slip along the tool, an additional continuous time delay is introduced in the model equations. Although the continuous time delay is significantly shorter than the discrete time delay, it may result in qualitative changes in the stability lobe diagrams. Thus, the improved stability behavior at low spindle speeds can be described by a multi-scale mechanism: by means of the interplay of the discrete time delay and the continuous time delay.

To verify the accuracy of the proposed model, external turning operations are performed on a CNC lathe (14.9 kW, 4500 rpm spindle). A rhombic carbide insert (KYS25) with the cutting tool holder (PCLNR2525M12) is employed to cut a workpiece of aluminum alloy ($Ø70 \times L250$ mm). The experimental setup is shown in Fig. 5. The rest of the equipment includes a B&K data acquisition box, a matching computer, and GRAS40pp micro-microphone with sensitivity of 50 mV/Pa to collect acoustic signals. During the cutting tests, chatter is measured using the machined surface finish and the microphone, whose signals are analyzed via fast Fourier transform (FFT) in order to observe the frequency content and compare it with the expected behavior of a stable cut to verify the predicted stability limits [38–41].

In the experiment, point A ($n = 300$ rpm, Kb = 1800 MN/m), point B ($n = 300$ rpm, Kb = 4200 MN/m), point C ($n = 740$ rpm, Kb = 4270 MN/m), and point D ($n = 740$ rpm, Kb = 850 MN/m) are selected from the stability lobe diagram to verify the accuracy of the proposed model. The processing parameters corresponding to point A from point D are used to machine the workpiece of aluminum alloy. Experiment results of external turning, workpiece surface and acoustic signals, are shown in Fig. 6 and Fig. 7, respectively.

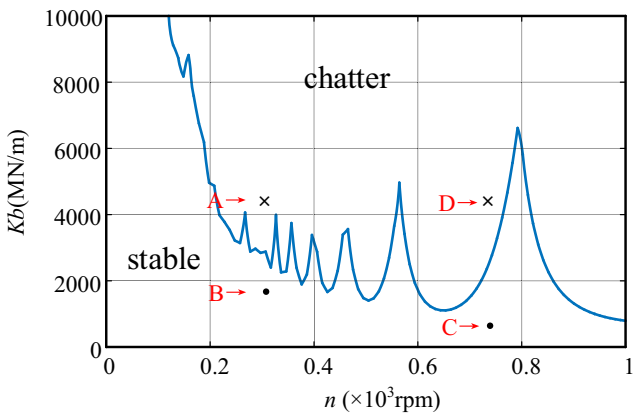

Fig. 4 Stability lobe diagram

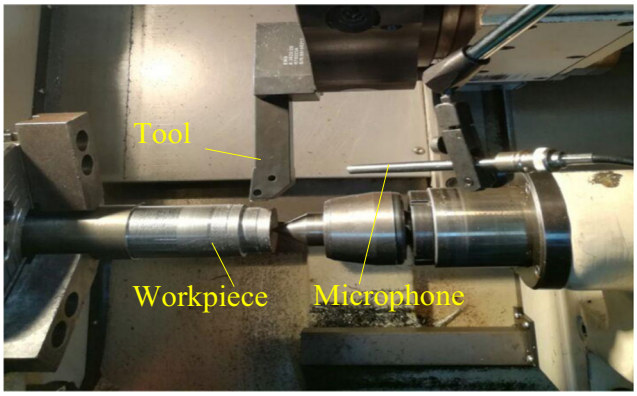

Fig. 5 The experimental setup

There is obvious vibration pattern in the machining area corresponding to point A and point D. By comparison, the turning process corresponding to point B and point C is stable according to the smooth machined surface finish. Since energy concentration in frequency domain is a key characteristic of chatter occurrence [42], chatter frequency is 1523 Hz at point A and 1496 Hz at point D, which obviously indicates there is chatter at point A and point D from Fig. 8. As a result, these experimental results verify the accuracy of the proposed model.

4.2 Parameter analysis

In the actual processing situation, q is impossible to equal to 0. Therefore, the distributed cutting force only with the short time delay on the stability of turning can be investigated by decreasing the value of q. The stability chart is shown in Fig. 9.

The stability lobe diagram shows that the distributed cutting force model, which includes both a discrete time delay and a continuous time delay, influences the stability of turning greatly, especially at low spindle speeds. For the distributed cutting force model only with a continuous time delay, the stability lobe diagrams show that when q keeps approaching 0, regions of stability are becoming greater and greater.

The parameter q is the ratio of the discrete time delay and the continuous time delay in the system, which can be expressed as the ratio of the circumference $d\pi$ of cylindrical workpiece and the length l of contact line of chip and the active face of tool. Therefore, the ratio q decreases along with the decrease of the contact length l when the diameter of workpiece is fixed (as shown in Fig. 10a). By comparison, when the contact length l is assumed as a constant, the ratio

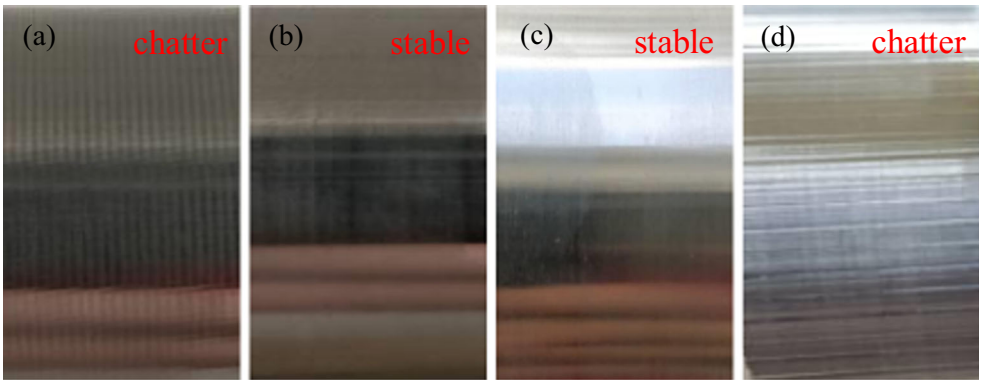

Fig. 6 Workpiece surface of (**a**) case A, (**b**) case B, (**c**) case C, and (**d**) case D

q increases along with the increase of the diameter of workpiece (as shown in Fig. 10b). As a result, chatter can be effectively avoided when the diameter of workpiece is larger and the contact length between tool and workpiece is shorter (as shown in Fig. 10c).

5 Conclusions

In this paper, a one-degree-of-freedom mechanical model is considered to describe chatter in turning operations with a distributed cutting force model, which is modeled as the resultant of a force system distributed along the rake face of the tool. An exponential shape function is used to approximate the force distribution on the tool–chip interface. The distributed force model results in a more complicated governing equation, a second-order delayed integrodifferential equation, which involves both a discrete time and continuous time delay. The continuous time delay results from a certain amount of time it takes the chip to slide along the rake face of the tool, while the discrete time delay is from the period between consecutive passages of the cutting tooth. An approach to transform and normalize the governing equation of motion into a third-order discrete system is described and the state-space representation of the new system is obtained. The semi-discretization method is used to compute the stability lobe diagrams of turning operations. In order to verify the accuracy of the proposed model, external turning operations of an aluminum alloy workpiece are performed on a CNC lathe. The accuracy of the proposed model can be verified to be correct

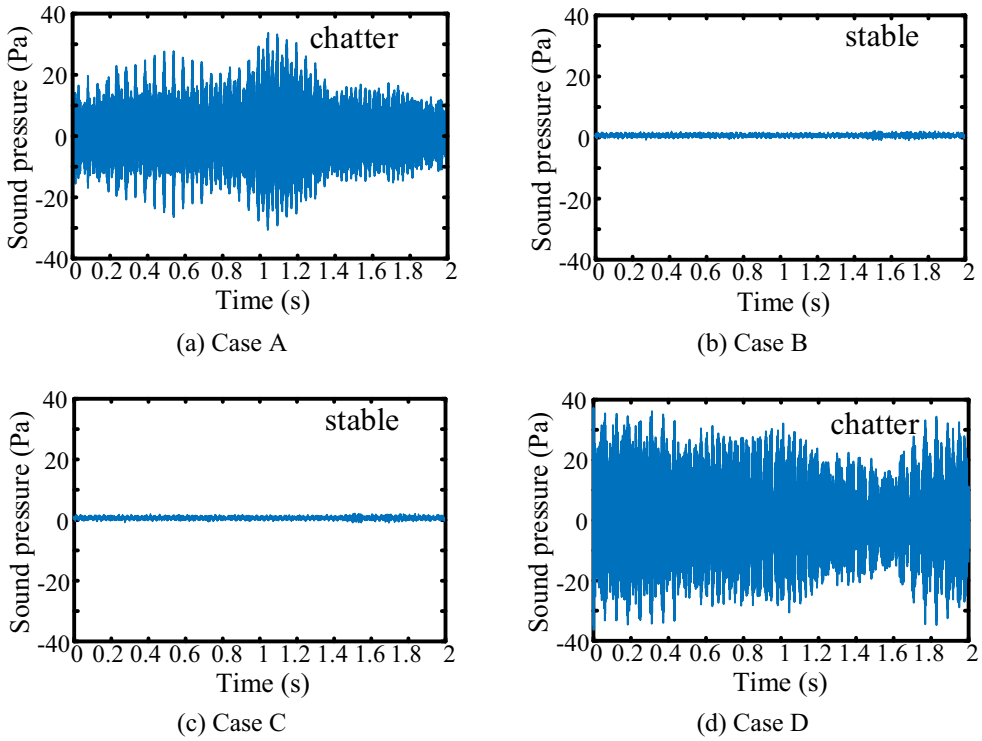

Fig. 7 Acoustic signals

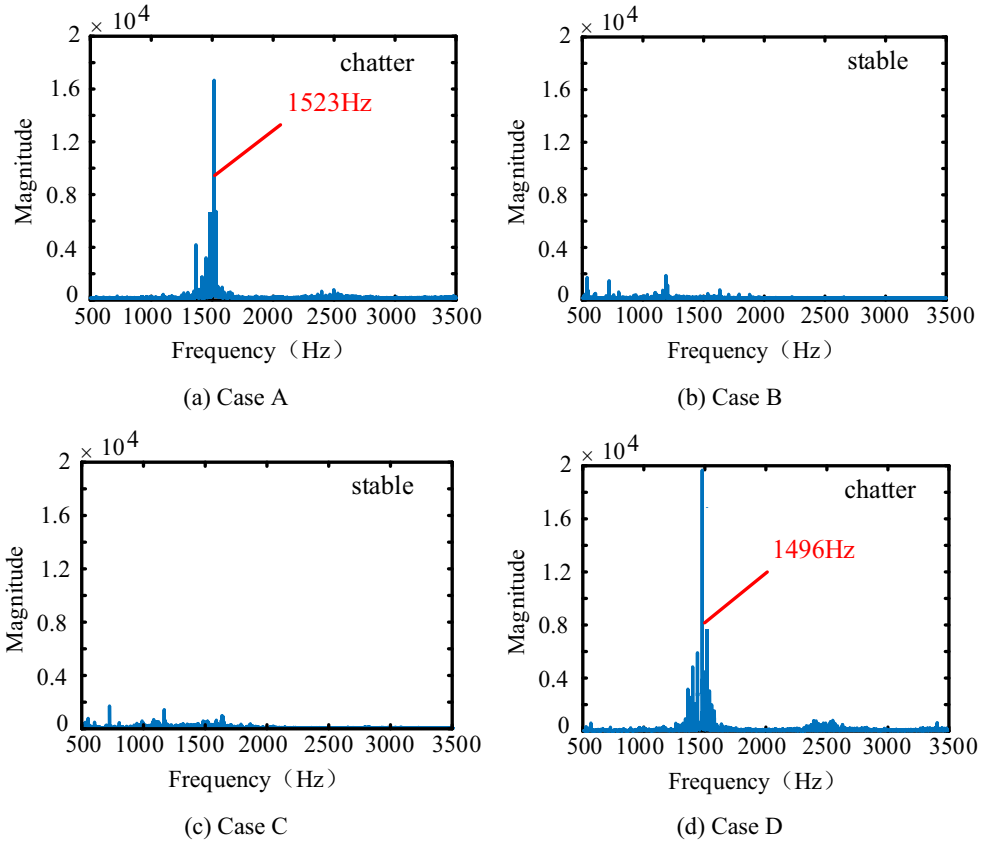

Fig. 8 FFT spectrum of acoustic signals

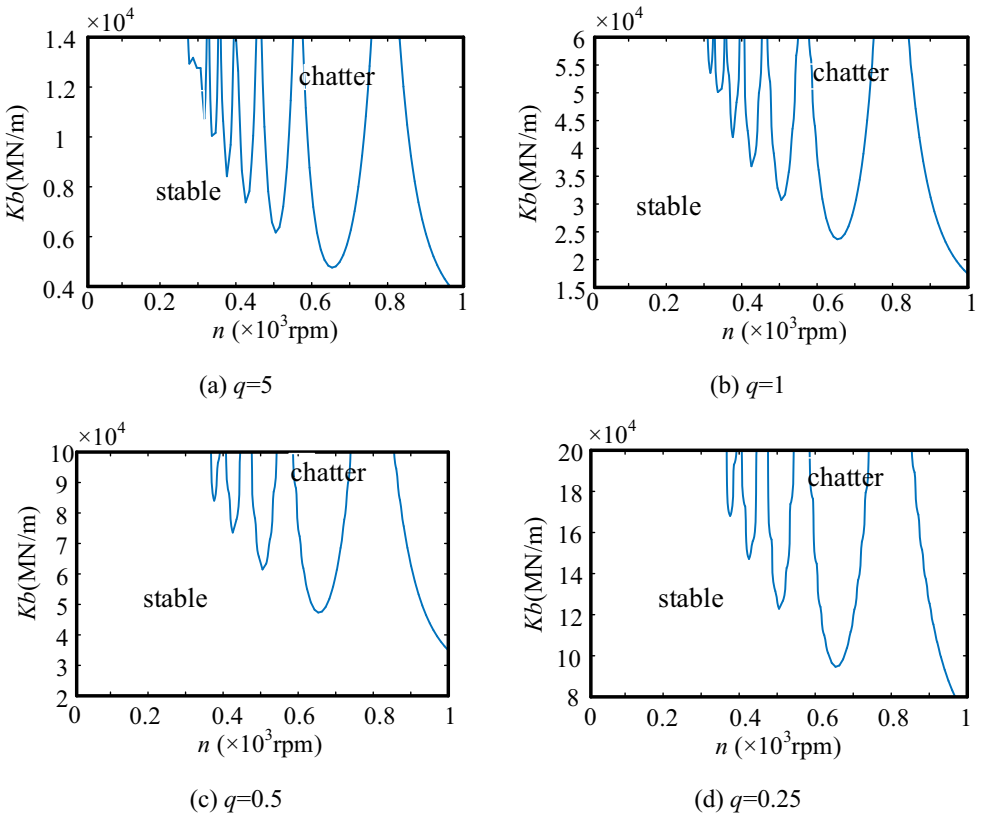

Fig. 9 Stability lobe diagrams

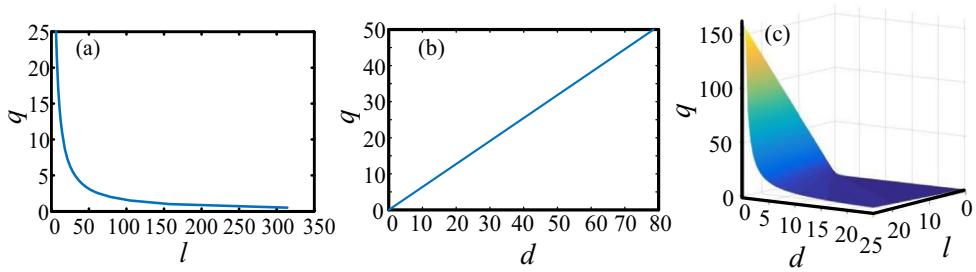

Fig. 10 The analysis of parameter q

from the workpiece surface and acoustic signals which are analyzed via FFT.

Moreover, contrary to the cutting force model with a discrete time delay and a continuous time delay, assume that the cutting force model only includes a continuous time delay to study the effect of the continuous time delay on the stability of turning. The results show that the continuous time delay has little influence on the stability of turning. When the workpiece diameter is larger and the contact length between tool and workpiece is shorter, the tool is more stable. Finally, constructing a solution strategy that can accommodate different shape functions for the force distribution and the contact length between the tool and the workpiece will be the subject of future research.

Funding information The authors received financial supports from the National Natural Science Foundation of China (no. 51575319, 51875320), Young Scholars Program of Shandong University (no. 2015WLJH31), the United Fund of Ministry of Education for Equipment Pre-research (no. 6141A02022116), and the Key Research and Development Plan of Shandong Province (no. 2018GGX103007).

Compliance with ethical standards

Conflict of interest The authors declare that they have no conflict of interest.

Publisher's Note Springer Nature remains neutral with regard to jurisdictional claims in published maps and institutional affiliations.

References

1. Song QH, Liu Z, Shi Z (2014) Chatter stability for micromilling processes with flat end mill. Int J Adv Manuf Technol 71(5–8): 1159–1174
2. Tobias SA (1965) Machine-tool vibration. Blackie
3. Altintas Y (2012) Manufacturing automation: metal cutting mechanics, machine tool vibrations, and CNC design. Cambridge University Press
4. Zhang XW, Yu T, Wang W (2016) Chatter stability of micro end milling by considering process nonlinearities and process damping. Int J Adv Manuf Technol 87:2785–2796
5. A.K. Firas, P.M. Brian (2009) Increased stability of low-speed turning through a distributed force and continuous delay model. J Comput Nonlin Dynam 4(4): 041003–041001–12
6. Song QH, Ai X, Guo B (2012) Stability of turning process with a continuous delay model. Adv Mater Res 500:20–25
7. T.G. Molnár, T. Insperger, S.J. Hogan, G. Stépán (2016) Estimation of the bistable zone for machining operations for the case of a distributed cutting force model. J Comput Nonlin Dynam 11: 051008–051001–10
8. X.Z. Huang, M.W. Hu, Y.M. Zhang, C.M. Lv (2016) Probabilistic analysis of chatter stability in turning. Int J Adv Manuf Technol 87: 1–8
9. Molnár TG, Insperger T, Stépán G (2016) State-dependent distributed-delay model of orthogonal cutting. Nonlinear Dynam 84(3):1–10
10. Ozturk E, Comak A, Budak E (2016) Tuning of tool dynamics for increased stability of parallel (simultaneous) turning processes. J Sound Vib 360:17–30
11. Gyebrószki G, Bachrathy D, Csernák G, Stepan G (2018) Stability of turning processes for periodic chip formation. Adv Manuf 2018: 1–9
12. A. Comak, Y. Altintasb (2018) Dynamics and stability of turn-milling operations with varying time delay in discrete time domain. J Manuf Sci Eng 140: 101013-1-14
13. Dorlin T, Fromentin G, Costes JP (2016) Generalized cutting force model including contact radius effect for turning operations on Ti6Al4V titanium alloy. Int J Adv Manuf Technol 86(9–12): 3297–3313
14. Kim DY, Kim DM, Park HW (2018) Predictive cutting force model for a cryogenic machining process incorporating the phase transformation of Ti-6Al-4V. Int J Adv Manuf Technol 96:1293–1304
15. Ma LJ, Yu AB, Chen J (2017) Theoretical model of cutting force in turning the lithium disilicate glass-ceramic. Int J Adv Manuf Technol 92(9–12):4355–4366
16. Cao GJ, Wang Y, Tang G (2018) Properties of NiCrAlY coatings fabricated on superalloy GH4169 by electrospark deposition. Int J Adv Manuf Technol 96:1787–1793
17. H. Takahashi, T. Yuki, K. Suzuki (2016) Modeling of ball screw driven stage for drilling machines with lumped parameter system model and FEM model. Mech Eng J 3(4): 00068–00061–12
18. Slavik A (2012) Dynamic equations on time scales and generalized ordinary differential equations. J Math Anal Appl 385(1):534–550
19. Molnar TG, Insperger T (2015) On the effect of distributed regenerative delay on the stability lobe diagrams of milling processes. Period Polytech Mech Eng 59(3):126–136
20. Song QH, Shi J, Wan ZL (2016) A time-space discretization method in milling stability prediction of thin-walled component. Int J Adv Manuf Technol 89(9–12)
21. Dong XF, Zhang W, Deng S (2016) The reconstruction of a semi-discretization method for milling stability prediction based on Shannon standard orthogonal basis. Int J Adv Manuf Technol 85: 1501–1511
22. Borkovic A, Kovacevic S (2018) Rotation-free isogeometric analysis of an arbitrarily curved plane Bernoulli-Euler beam. Comput Method Appl M 334:238–267

23. Astakhov VP, Outeiro JC (2005) Modeling of the contact stress distribution at the tool–chip interface. Mach Sci Technol 9(1):85–99
24. Kilic DS, Raman S (2007) Observations of the tool-chip boundary conditions in turning of aluminum alloys. Wear 262(7–8):889–904
25. Boudelier A, Ritou M (2018) Cutting force model for machining of CFRP laminate with diamond abrasive cutter. Production Eng 12: 279–287
26. Kilic ZM, Altintas Y (2016) Generalized mechanics and dynamics of metal cutting operations for unified simulations. Int J Mach Tool Manu 104:1–13
27. Kim P, Seok J (2012) Bifurcation analyses on the chatter vibrations of a turning process with state-dependent delay. Nonlinear Dynam 69(3):891–912
28. Stepan G, Dombovari Z (2011) Identification of cutting force characteristics based on chatter experiments. CIRP Ann-Manuf Techn 60(1):113–116
29. Xu W, Wu XR, Yu Y (2017) Weight function, stress intensity factor and crack opening displacement solutions to periodic collinear edge hole cracks. Fatigue Fract Eng M 40:2068–2079
30. Astakhov VP, Outeiro JC (2005) Modeling of the contact stress distribution at the tool-chip interface. Mach Sci Technol 9(1):85–99
31. Buchkremer S, Klocke F, Lung D (2015) Finite-element-analysis of the relationship between chip geometry and stress triaxiality distribution in the chip breakage location of metal cutting operations. Simul Model Pract Th 55:10–26
32. Boujelbene M (2018) Investigation and modeling of the tangential cutting force of the titanium alloy Ti-6Al-4V in the orthogonal turning process. Procedia Manuf 20:571–577
33. Lu KB, Lian ZS, Gu FS (2018) Model-based chatter stability prediction and detection for the turning of a flexible workpiece. Mech Syst Signal Process 100:814–826
34. Kumar S, Singh B (2018) Prediction of tool chatter and metal removal rate in turning operation on lathe using a new merged technique. J Braz Soc Mech Sci 40(2):53–63
35. Song QH, Ai X, Tang WX (2011) Prediction of simultaneous dynamic stability limit of time-variable parameters system in thinwalled workpiece high-speed milling processes. Int J Adv Manuf Technol 55(9–12):883–889
36. Kim HS, Ehmann KF (2016) A cutting force model for face milling operations. Int J Mach Tool Manu 33(5):651–673
37. Dikshit MK, Puri AB, Maity A (2017) Chatter and dynamic cutting force prediction in high-speed ball end milling. Mach Sci Technol 21(2):291–312
38. Zhang XW, Yu TB, Wang WS (2018) Prediction of cutting forces and instantaneous tool deflection in micro end milling by considering tool run-out. Int J Mech Sci 136:124–133
39. Jauregui JC, Resendiz JR, Thenozhi S, Szalay T (2018) Frequency and time-frequency analysis of cutting force and vibration signals for tool condition monitoring. IEEE Acess 6(99):6400–6410
40. Gao J, Song QH, Liu Z (2018) Chatter detection and stability region acquisition in thin-walled workpiece milling based on CMWT. Int J Adv Manuf Technol 2018:1–15
41. Luo M, Luo H, Axinte D, Liu D, Mei J, Liao Z (2018) A wireless instrumented milling cutter system with embedded PVDF sensors. Mech Syst Signal Process 110:556–568
42. Khasawneh FA, Munch E (2016) Chatter detection in turning using persistent homology. Mech Syst Signal Process 70-71:527–541